Combustion and Radiation Characteristics of Oxygen-Enhanced Inverse Diffusion Flame

Sang Soon Hwang*
Department of Mechanical Engineering University of Incheon, Dohwa-dong, Nam-ku Incheon 402-749, Korea
Jay P Gore
School of Mechanical Engineering Purdue University West Lafayette, USA

The characteristics of combustion and radiation heat transfer of an oxygen-enhanced diffusion flame was experimentally analyzed. An infrared radiation heat flux gauge was used to measure the thermal radiation of various types of flames with fuel, air and pure oxygen. And the Laser Induced Incandescence (LII) technique was applied to characterize the soot concentrations which mainly contribute to the continuum radiation from flame. The results show that an oxygen-enhanced inverse diffusion flame is very effective in increasing the thermal radiation compared to normal oxygen diffusion flame. This seems to be caused by overlapped heat release rate of double flame sheets formed in inverse flame and generation of higher intermediate soot in fuel rich zone of oxygen-fuel interface, which is desirable to increase continuum radiation. And the oxygen/methane reaction at slight fuel rich condition ($\phi=2$) in oxygen-enhanced inverse flame was found to be more effective to generate the soot with moderate oxygen availability.

Key Words : Oxygen-Enhanced Inverse Diffusion Flame, Radiation Heat Transfer, Laser Induced Incandescence

1. Introduction

Recently, manufacturing processes that need high heat or mainly use radiation heat transfer (glass manufacturing, billet manufacturing in the iron mill, ladle heating, etc.) tend to change their fuel from fuel oil to liquefied natural gas (LNG) which costs low with low emission and is easy to store and carry.

Most manufacturing processes use turbulent diffusion flames to obtain the desired radiation heat flux. This radiation heat flux of diffusion flame is generally provided by the two radiation sources which consist of luminous flame radiation from soot and to some extent, non-luminous flame radiation from the combustion products, CO_2 and H_2O. The radiation fraction in total heat transfer of the diffusion flame varies from a few percent to greater than 90% according to the type of fuel and the flow condition (Baukal, 1997).

However, methane which contains more than 80% of LNG produces a low amount of soot resulting in lower radiation heat transfer (Turns, 1996). For this low sooting flame, the generation of the high intermediate soot could be one of ways to increase the radiant heat transfer. Oxygen-enhanced methane flame was chosen in this study since it has high radiation heat transfer caused by the increase of soot formation mostly in the rich mixture ratio and its high heating rate due to high adiabatic flame temperature.

There have been several researches on radiation heat transfer of air/fuel flame which have deve-

* Corresponding Author,
E-mail : hwang@lion.inchon.ac.kr
TEL : +82-32-770-8417
Department of Mechanical Engineering University of Incheon, Dohwa-dong, Nam-ku Incheon 402-749, Korea. (Manuscript **Received** September 13, 2001; **Revised** May 27, 2002)

loped successful methods for radiation properties if temperature, soot volume fraction and gas concentrations are known or can be predicted (Gore & Faeth, 1986; Sivanthanu et al., 1991; Sivanthanu & Gore, 1992; Gore et al., 1999; Zheng & Gore, 2001).

Neverthless, studies on oxygen-enhanced flame was not motivated enough in spite of relative importance of radiation of oxygen-enriched flame. This was mainly because the oxygen manufacturing cost was very expensive. The oxygen is, however, recently becoming economically feasible due to the development of cost effective oxygen manufacturing process. This has motivated many studies of the oxygen/fuel combustion. The characteristics of soot formation of oxygen/fuel flame was recently studied by Sergei et al (2000) and Beltrame et al (2001). Sergei et al (2000) investigated the relative effects of acetylene and PAH on soot formation in laminar oxygen/methane flame. They found that the effect of PAH addition on soot growth became substantially stronger with oxygen enrichment. The soot and NO formation in the oxygen/methane diffusion flames was studied by Beltrame et al (2001) experimentally and computationally. They showed that oxygen variation significantly modified the diffusion flame structure and flame temperature, resulting in a substantial increase of soot.

Since soot distribution of oxygen/fuel flame is closely related to radiant heat transfer, the characteristics on the radiant heat transfer of oxygen/fuel flame and role of soot have become a subject of increasing interest (Chales et al., 1997).

In this work, several combinations of air/methane and oxygen/methane flames are analyzed in order to find which type of oxygen-enhanced flame produces high intermediate soot and makes use of the high temperature capability of oxygen-enriched combustion. Especially the effects of flow field configurations on the radiation heat transfer of normal and inverse coflowing air/fuel and oxygen/fuel flame are compared and analyzed.

For this purpose, the radiation heat flux meter is used to characterize the radiation properties and LII (Laser Induced Incandescence) is applied to detect instantaneously the soot which is considered to be the primary source of the luminous radiation.

2. The Characteristics of Oxygen-Enhanced Flame

2.1 High flame temperature of the oxygen flame

The amount of pure oxygen participating in combustion process is characterized by **P** (Oxy gen Participation) defined as pure oxygen fraction of total amount of oxygen required.

$$P\,(Oxygen\ Participatin)=\frac{PureOxygen}{PureOxygen+0.21Air}$$

Figure 1 shows the adiabatic flame temperature as a function of oxygen addition (P). It can be seen that the adiabatic flame temperature of the pure oxygen-methane (P=1) flame is 3076 K, which is about 800 K higher than that of the air-methane (P=0) flame. This high temperature flame tends to increase the radiation energy significantly. And the oxygen/methane flame maintains high temperature from a slight rich to lean equivalence ratio while its temperature decreases rapidly as equivalence ratio increases.

2.2 The increase of radiation heat transfer

Figure 2 represents the mole concentration of

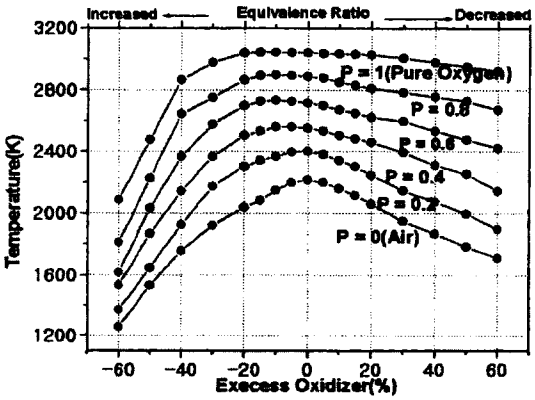

Fig. 1 Adiabatic Flame Temperature of Methane-Oxygen Flame (Program STANJAN for chemical equilibrium calculations was used)

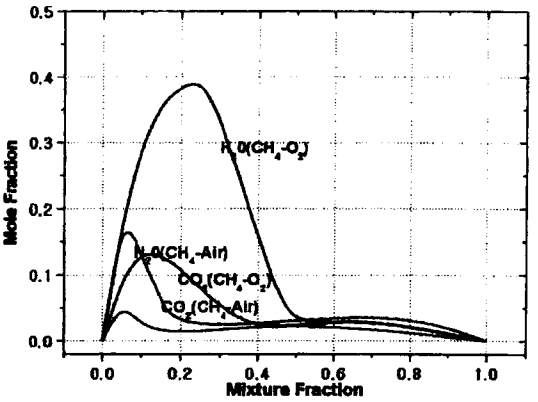

Fig. 2 Mole Fraction of CO_2 and H_2O in Methane-Air/Methane-Oxygen Flame (Program PREPDF2.4 calculations was used)

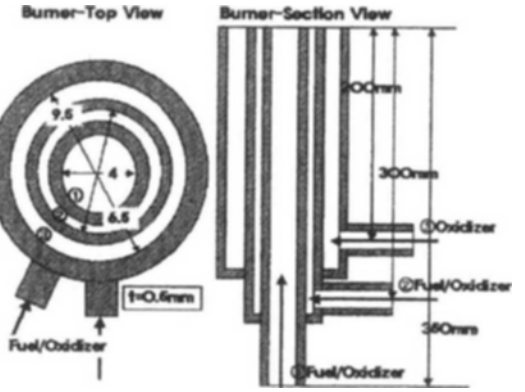

Fig. 3 Schematic diagram of double concentric burner

the combustion products produced during oxygen-enriched combustion. From the figure, the oxygen-methane flame shows much higher concentrations of CO_2 and H_2O compared to the air-methane flame. The increased temperature and partial pressures of CO_2 and H_2O lead to an increase in molecular radiation (Baukal, 1997).

According to the work of Baukal (1997), high amounts of soot are produced in the fuel rich regions of oxy-fuel flames. This large amount of soot contributes to the continuum radiation from the flame.

The disadvantages of oxygen-enriched flame are the reduction in convection heat transfer caused by the small amount of burnt gas (the reduction of the amount of N_2), and the increase in operational costs (the additional cost of using oxygen). However, it is adequate in some applications which utilize purely radiant heating and require higher temperature.

3. Method of Experiment

3.1 The burners

The burner used in this work is shown in Fig. 3. The burner was designed by adopting Moss experiment (Brookes & Moss, 1999) and through many preliminary tests using burners of different sizes in order to make a turbulent flame from the estimation of Reynolds number of each flame. Many combination of methane, oxygen, air, and air + oxygen were introduced into each of the burner nozzles to make different types of diffusion flames. The Reynolds numbers of the various cases are different. But the fuel flow rate is maintained constant and the oxygen flow rate is changed regarding equivalence ratio of methane and oxygen. This is the proper comparison from practical standpoint although the flow fields are different.

3.2 The measurement of thermal radiation heat flux

The radiation heat flux was measured using PASCO's radiometer (model TD-8549). The wavelength range of this radiometer, which spans the whole range of the infrared rays, is 0.6~30.0 μm and its sensitivity is 20 $\mu m/cm^2$. As shown in Fig. 4, by restricting the view angle of the radiometer to $\theta=7.5$ using a view-restrictor with a water-cooling body, only the radiation from a measurement point on the flame was detected. The temperature of the view-restrictor with the water-cooling body was controlled to maintain about 300 K using the T-type thermocouple.

The effectiveness of the view restrictor was checked by measuring radiation heat flux as a function of distance from the flame. Figure 5 shows the variation of radiation heat flux as a function of distance from the flame normalized by the width of the visible flame. There is very little

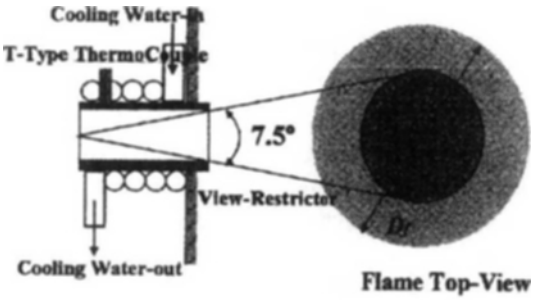

Fig. 4 View-restrictor

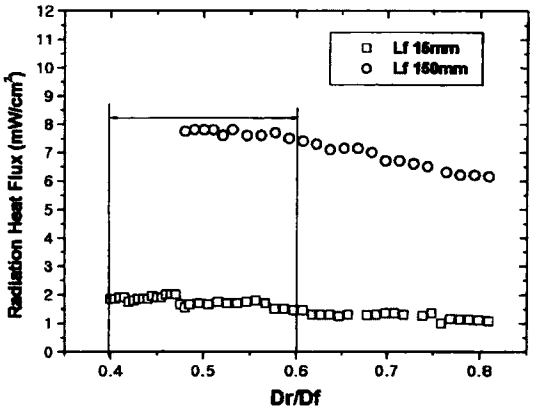

Fig. 5 Measurement of radiation heat flux as function of Dr/Df ratio (DIFP05, P=0.5, ϕ=1.0, Qr=3.327 kw)

variation in the radiation heat flux measured between Dr/Df=0.4~0.6. Therefore, the measuring locations were set to Dr/Df=0.5.

3.3 The 2D plane distribution characteristics of soot obtained LII (Laser Induced Incandescence) technique

To investigate the characteristics of soot distribution that may contribute a large part of the radiation heat transfer in the diffusion flame, the LII (Laser Induced Incandescence) technique was used. The LII technique can measure the instantaneous soot concentration in turbulent flame. Its technique is based on the fact that the intensity of incandescent radiation is in proportion to soot concentration (Melton, 1984). The soot is heated to incandescence temperature of above 4,000 K by a high energy density laser beam for a few nanoseconds. Its advantage is that it can measure the concentration and the particle size distribution of the soot particles in nearly real-time. To simplify the interpretation of the results, it is assumed that laser sheet has the same energy flux.

The second harmonic frequency (532 nm) of Nd : Yag laser was used as measuring frequency of LII method. Laser power and pulse duration time were 254 mJ/pulse and 7 ns respectively. A 25.4×25.4 mm cylindrical lens and a spherical lens with a diameter of 101.6 mm were arranged to obtain a laser sheet of 100 mm in height and 0.5 mm in width. LII measurement was made using an ICCD camera with 400 nm filter to avoid the fluorescent noise induced by C_2. The gate time of the ICCD camera was set at 100 ns to minimize the effects of background noise.

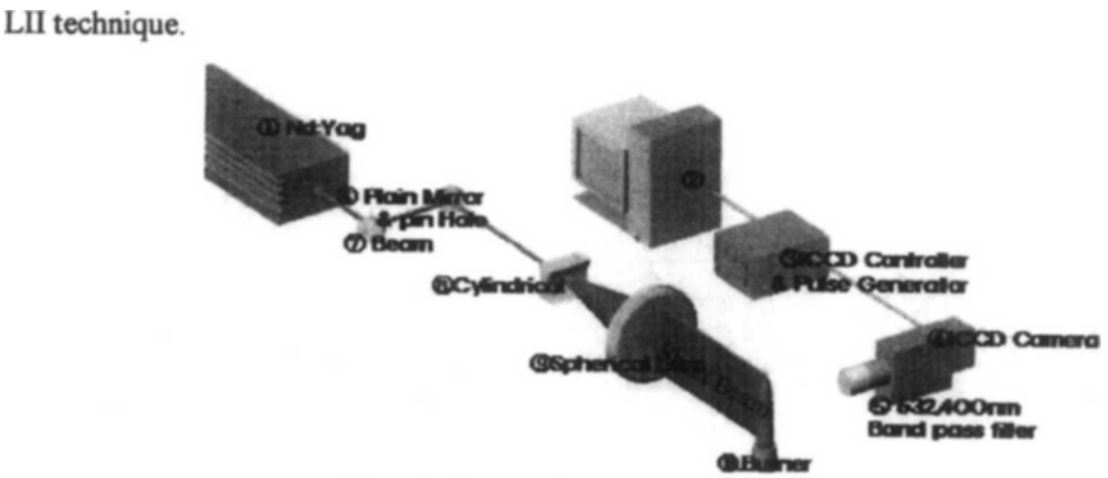

Fig. 6 Schematic diagram of LII experimental apparatus

Figure 6 depicts the experimental diagram of the soot distribution measurement apparatus using the LII technique.

4. Results and discussions

Four types of flames as shown in Fig. 7 were studied. The first type involves normal diffusion flame with fuel supplied through the central port (NDF) and second with fuel flowing from an annulus into still air (ADF). The third type is an oxygen/fuel diffusion flame with fuel flowing through a central port and oxygen flowing into outer annulus (OADF). Fourth type has the flame with oxygen flowing through central port and fuel supplied into outer annular port (OIDF). The flow rate of each gases is controlled by precision electronic mass flow meter with accuracy better than 1%.

The test conditions for these different flame types are listed in Table 1.

4.1 Reference Flames (fuel flow only) Diffusion Flame (NDF) and the Annular Diffusion Flame (ADF)

It is important to know the radiation characteristics of normal diffusion flame and annular diffusion flame in which only fuel flows in still air as reference flames of oxygen-enhanced flame. These help to know which location of fuel flow, i. e mixing direction of fuel and oxidant, gives more intense radiation heat transfer.

Photographs of Fig. 8 show that the ADF is visibly wider and shorter than the NDF. Figure 8 (c) shows the instantaneous soot distribution in the region marked by a square in ADF measured by LII. The LII images at 10 cm height above nozzle are plotted. The soot particles are distributed in the form of ligaments around the yellow colored flame sheet.

Figure 9 shows the total radiation heat flux parallel to the axis of the two flames with an identical firing rate (Qr=3,33 kW) measured by radiometer. The distance between the heat flux gauge and the flame axis is set at 15 cm. There is no variation of output signal above 15 cm distance. The mean and the maximum radiation intensity of the ADF is seen to be higher than that of the NDF showing that the fuel supplied through the outer annular tube instead of the central tube produces a higher radiation heat flux.

Table 1 Summary of test conditions (Φ=1 in case of the OADF and the OIDF)

Flame Type	NDF	ADF	OADF	OIDF
Reynolds number*	1,690	422	1,690	422
Velocity(Central tube) (m/s)	6.63	-	6.63	14.32
Velocity(Annular tube) (m/s)	-	6.15	13.28	6.15
Heat release rate(kW)	3,327	3,327	3,327	3,327
Fuel flow rate(l/min)	5	5	5	5
Oxygen flow rate(l/min)	0	0	10	10

*Reynolds number based on fuel flow

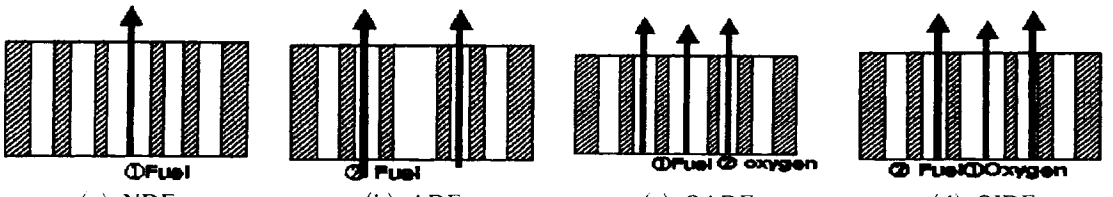

(a) NDF (b) ADF (c) OADF (d) OIDF

Fig. 7 The type of burner with combination of Fuel and Oxidizer

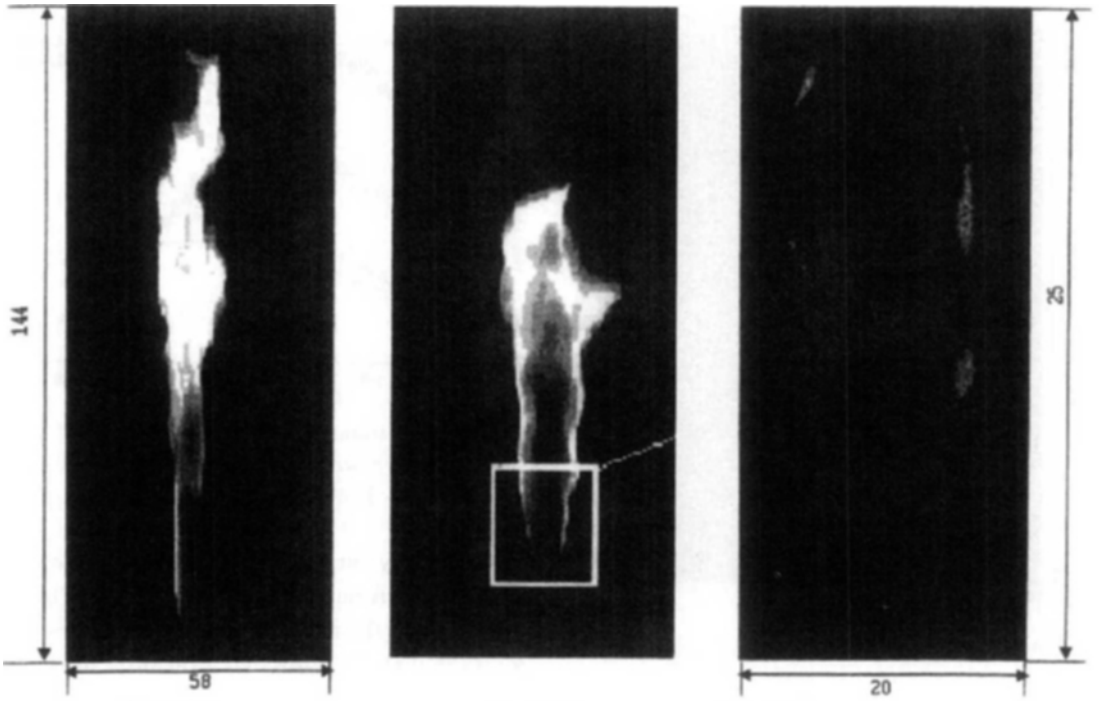

Fig. 8 Photography and soot distribution of NDF, ADF (Qr=3.327 kw)

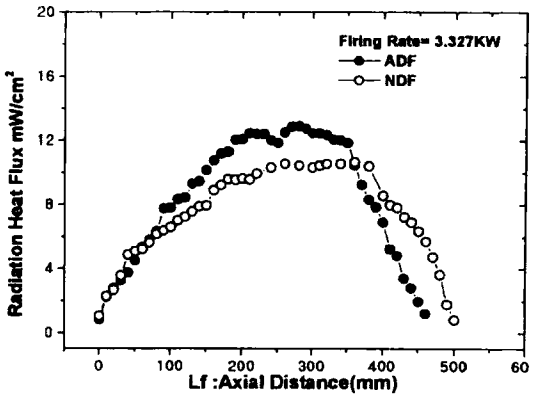

Fig. 9 Comparison of Radiation Heat Flux results with NDF, ADF (Qr=3.327 kw)

4.2 Oxygen-enhanced Diffusion Flame : Oxygen Annular Diffusion Flame (OADF) and Oxygen Inverse Diffusion Flame (OIDF)

Based on above results, experiments were conducted to study the effects of the location of fuel and oxygen flows in oxygen-enhanced flame. It is known that oxygen-enhanced combustion produces the increased temperature and partial pressures of CO_2 and H_2O which lead to an increase in gas band radiation. In addition, high amount of soot is produced in the fuel rich regions of oxygen-enhanced flame which contribute to the continuum radiation from the flame. It is very important to make the suitable combustion mode which takes advantage of above radiation properties of oxygen-enhanced flame.

During this experiment, the fuel flow rate was set to constant value as in NDF and ADF and equivalence ratio based on oxygen was set to 1. From OADF of Fig. 10, luminous area is observed to be distributed on entire flame surface similar to the case of normal diffusion flame. From LII signal, a little more ligaments of soot than those of air/fuel flame as ADF in Fig. 8 appears around the flame sheet. This soot formation and higher flame temperature of oxygen-fuel flame are likely to contribute to make it more luminous. The flame photograph and instantaneous soot distribution of OIDF are presented in Fig. 11. It is distinguishable that the very lumi-

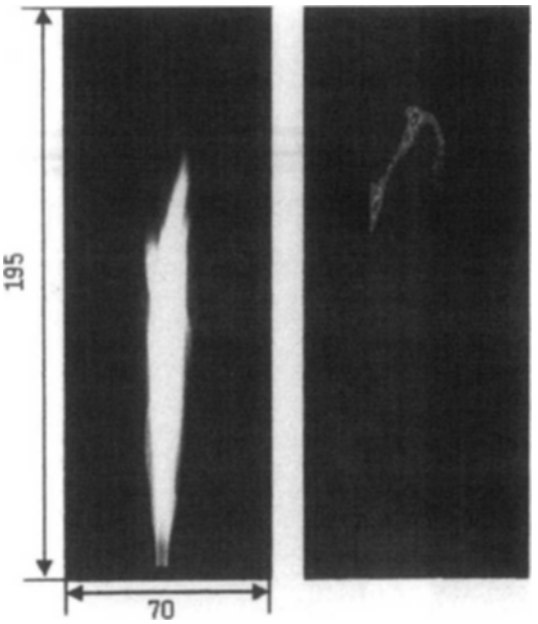

Fig. 10 photography of OADF and instantaneous soot distribution (Qr=3.327 kw, P=1.0, Φ=1.0)

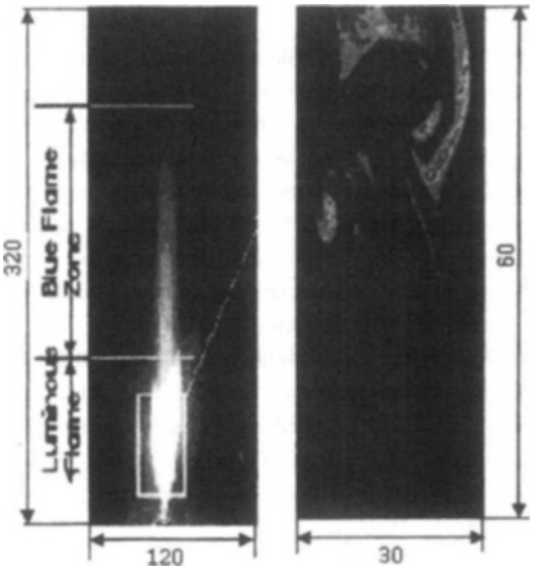

Fig. 11 Photography of OIDF and instantaneous soot distribution (Qr=3.327 kw, P=1.0, Φ=1.0)

nous part of flame is shifted to the bottom of the flame and blue flame is observed in the upper side of flame. The radiation intensity of this luminous

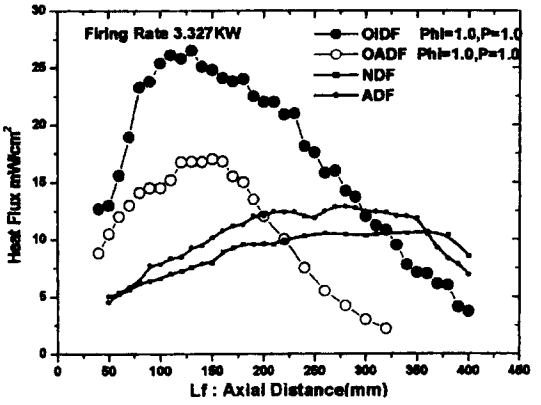

Fig. 12 Radiation heat flux results of OIDF and OADF with comparison of NDF and ADF (Qr=3.327 kw)

part is visibly very strong. The LII image of the most luminous part of flame is plotted in Fig 11. It shows that the multiple size of soot eddies like eddies in turbulent flows are evident in the luminous part of flame. It is thought that this strong radiation is caused by the continuum radiation of the multiple eddies of soot as well as the increased gas band radiation. This result implies that the inverse diffusion flame is more effective to create the inflame soot in oxygen/fuel flame.

Figure 12 depicts the comparison of the overall radiation heat flux of the OADF and the OIDF with identical amount of oxygen and fuel as a function of the distance from the burner exit (Lf). The axial radiation heat fluxes of the NDF and the ADF are also shown as reference. The maximum heat flux of the OIDF is about twice that of the ADF. The OIDF produces much higher heat flux than that of the OADF along the flame axis. These characteristics could be explained using the schematic flame structure diagram of Fig 13. In case of OADF, the oxygen surrounds the fuel as shown in Fig. 13(a), while in the case of OIDF the fuel surrounds the inner oxygen as shown in Fig. 13(b). In the latter case, an inner flame sheet of high temperature is formed by the inverse diffusion reaction between fuel and the oxygen and an outer reaction sheet is formed by the reaction between the fuel and the surrounding air. Therefore, these double flame sheets augment the heat release rate and the radiation

heat flux of the flame with the effects of the higher intermediate soot formation of OIDF mentioned above. This flame structure could be also used to explain the reason that the ADF has higher heat flux than the NDF in air-methane flame.

Now it is important to know the effect of amount of the oxygen supply in OIDF on the radiation heat flux since the use of oxygen means the additional cost of expense. The increase in the amount of oxygen corresponds to a decrease of equivalence ratio, Φ and thus the amount of pure oxygen can be expressed as value of Φ. Figure 14 shows the flame photography and accumulated soot distribution at $\Phi=2$ and 4 measured at the most luminous part of each flame. In case of $\Phi=4$, the flame is similar to normal diffusion flame shown in Fig. 14(b). Its luminous region is distributed on entire flame sheet and yellow in color. But as Φ decreases to $\Phi=2$ (Fig. 14 (a)), very luminous zone becomes to appear ($100\ \text{mm} \leq Lf \leq 200\ \text{mm}$) in the lower part of the flame and is maintained at almost same location even if Φ becomes less than 2.0.

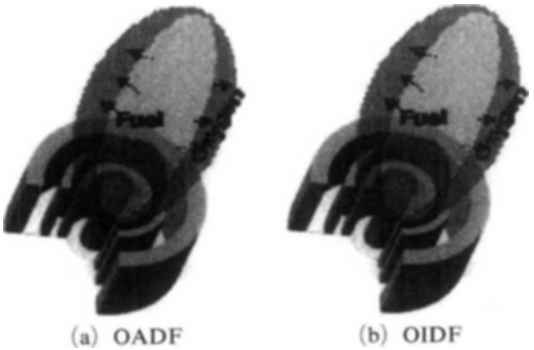

(a) OADF (b) OIDF

Fig. 13 Schematic of Flame Structure of OADF and OIDF

The flame length measurement result of Fig. 15 shows that the flame length is the shortest near $\Phi=2$, regardless of the heat release rate (Qr). It seems that more active reaction occurs at the condition of approximately $\Phi=2$. Within the

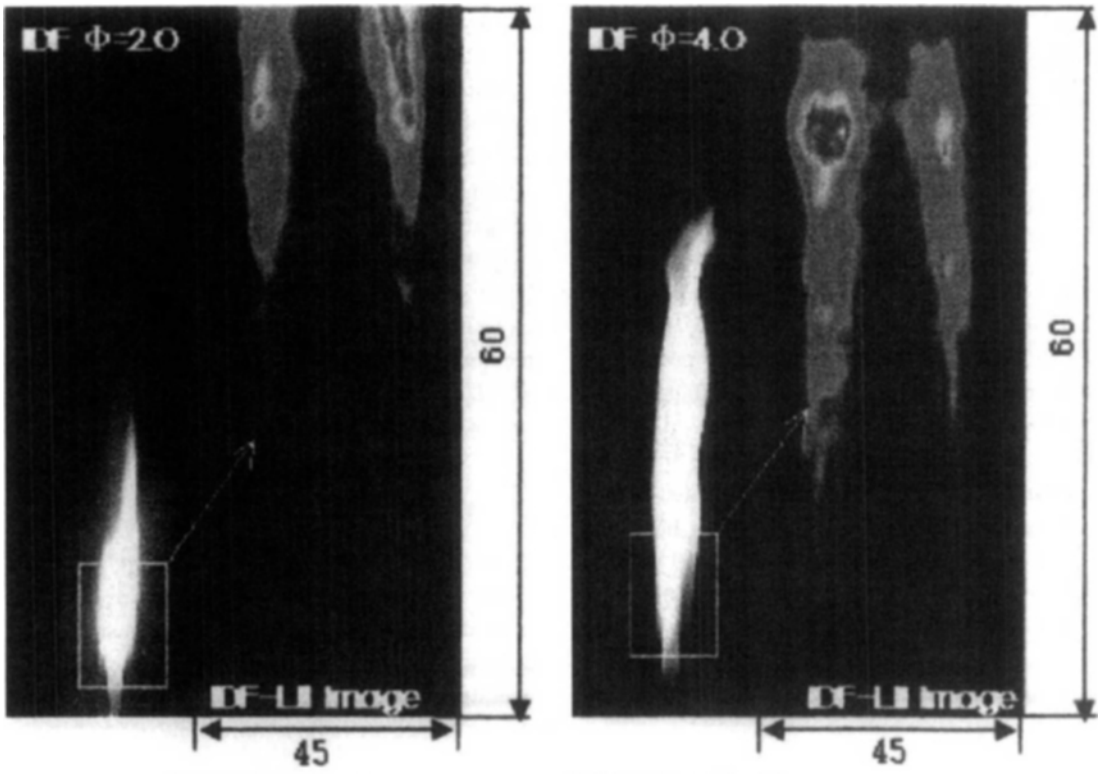

(a) OIDF at $\Phi=2.0$ (b) OIDF at $\Phi=4.0$

Fig. 14 Flame and averaged soot distribution of OIDF at $\Phi=2$ and 4 (Qr=3.327 kw, P=1.0)

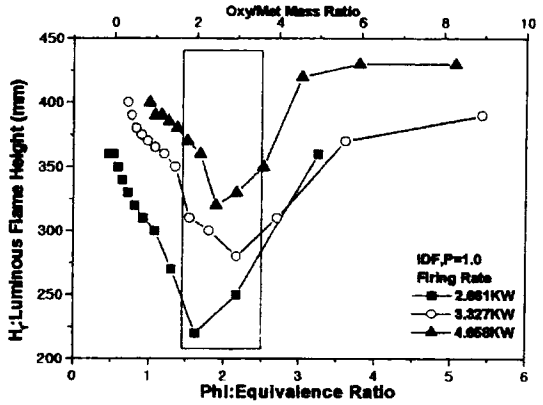

Fig. 15 Comparison of Luminous flame height of OIDF at different Qr (P=1.0)

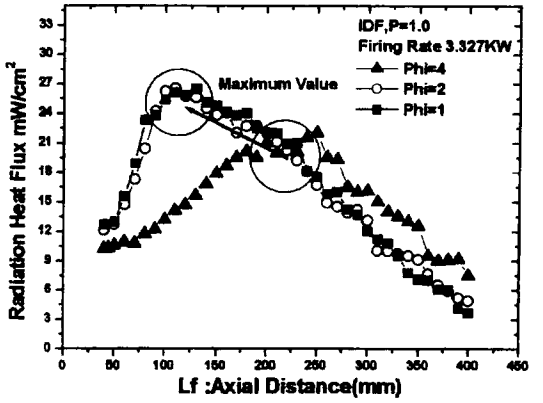

Fig. 16 Axial distribution of radiation heat flux of IDF at different Φ

range of $\Phi<2$ (Fig. 11 and Fig. 14 (a)), this luminous region is at almost constant size but the overall length of the flame increases because of the increase of the length of the blue flame in the upper part of the flame.

The axial profiles of radiation heat flux as a function of equivalence ratio are presented in Fig. 16. The maximum value of radiation heat flux moves toward the lower part of the flame and has higher value as Φ is decreased from 4.0 to 1.0. Interestingly, it is found that in ranges where $\Phi<2$ (increase of oxygen) the axial profiles and the maximum value of radiation heat flux are almost same.

Figure 17 shows the effects of equivalence ratio on the mean and maximum radiation heat flux of the OIDF. It is found that the mean and maximum radiation heat transfer increases generally by the increase in the amount of pure oxygen (decrease of Φ), but in case the amount of pure oxygen exceeds the amount of oxygen that corresponds to $\Phi=2$, there is not any noticeable difference of the radiation heat flux, which means that there exists a limit in the value of pure oxygen necessary for the increase of radiation heat flux.

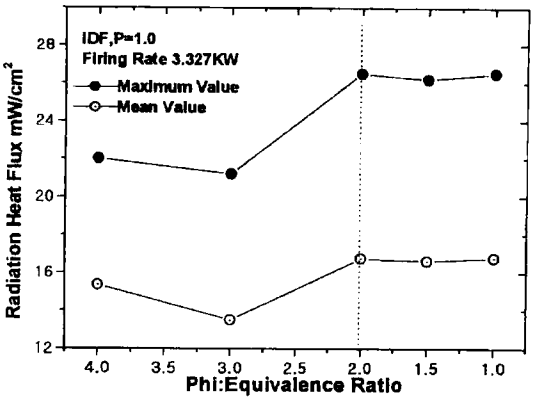

Fig. 17 Radiation heat fluxes of OIDF as a function of Φ (Qr=3.327 kw, P=1.0)

Above results also suggest that oxygen/methane reaction at slight fuel rich condition ($\Phi=2$) seems to be effective to generate more intermediate soot with moderate expense of oxygen.

In the view of fuel saving, the fuel savings using OIDF estimates to about 36% when the cost of oxygen/LNG corresponds to 0.266 because the maximum heat flux of OIDF is almost twice that of ADF and oxygen is consumed as same as fuel supply at the condition of $\Phi=2$.

5. Conclusions

(1) The oxygen inverse diffusion flame is found to be more effective in generating a strong radiant heat flux compared to oxygen normal diffusion flame. This seems to be caused by overlapped heat release rate of double flame sheets formed in inverse flame and more generation of intermediate soot in fuel rich zone of oxygen/fuel interface, which increases continuum radiation of the flame.

(2) The radiation heat flux of oxygen inverse diffusion flame maintains the almost same value at the equivalence ratio of less than 2 since soot region which largely contributes to continuum radiation of flame is kept at almost same size.

(3) The oxygen methane reaction at the slight rich condition ($\Phi=2$) of oxygen inverse diffusion flame is found to be desirable to generate much higher radiation heat flux with least use of oxygen.

Acknowledgment

The author greatly acknowledges to the financial support of the Korea Research Foundation Grant (KRF-2000-013-EA0011) and also thanks Professor S. H. Chung of Seoul National University for his support of LII measurement.

References

Baukal, C. E, 1997, *Oxygen Enhanced Combustion*, pp. 2~44.

Beltrame, A. et al., 2001, "Soot and NO Formation in Methane-Oxygenenhanced Diffusion Flames," *Combustion and Flame*, Vol. 124, pp. 295~310.

Brookes, S. J. and Moss, J. B., 1999, "Measurements of Production Thermal Radiation From Confined Turbulent Jet Diffusion Flames of Methane," *Combustion and Flame*, 116 : pp. 49~61.

Chales. E., Baukal, C. E. and Benjamin, 1997, "Oxygen-Enriched/Natural Gas Flame Radiation," *International Journal of Heat Transfer*, Vol. 40, No. 11, pp. 2539~2547

Gore, J. P. and Feath, G. M., 1986, "Structure and Spectral Radiation Properties of Turbulent Ethylene/Air Diffusion Flames," *Twenty-first Symposium (International) on Combustion/The Combustion Institute*, pp. 1521~1531.

Gore, J. P. et al., 1999, "A Study of the Effects of Thermal Radiation on the Structure of Methane/Air Counter-flow Diffusion Flames Using Detailed Chemical Kinetics," *Proceedings of the 5th ASME/JSME Joint Thermal Engineering Conference (CD)*, Paper AJTE99-6311, p. 50 (Book of Abstracts).

Melton, L. A., 1984, "Soot Diagnostics Based on Laser Heating," *Applied Optics*, 23, pp. 221~2208.

Sergei, A. Z. et al., 2000, "Relative Effect of Acetylene ans PSAHs Addition on Soot Formation in Laminar Diffusion Flames of Methane with Oxygen and Oxygen-Enriched Air," *Combustion and Flame*, Vol. 122, pp. 76~89.

Sivanthanu, Y. R. et al., 1991, "Transient Scalar Properties of Strongly Radiating Jet Flames," *Combustion Science and Technology*, Vol. 76, pp. 45~66.

Sivanthanu, Y. R. and Gore, J. P., 1992, "Transient Structure and Radiation Properties of Strongly Radiating Buoyant Flames," *Journal of Heat Transfer*, Vol. 114, pp. 659~665.

Turns, S. R., 1996, *An Introduction to Combustion*, pp. 291~295.

Zheng, Y. and Gore, J. P., 2001, "Time Series Simulation on Radiation from Turbulent CH4/H2/N2 Flames," *Proceedings of the Second Joint Meeting of the U. S. Sections of the Combustion Institute (CD)*.